Fabrication of nanomagnet arrays by shadow deposition on self-organized semiconductor substrates

C. Teichert,[a] J. Barthel, H. P. Oepen, and J. Kirschner
Max-Planck-Institut für Mikrostrukturphysik, Weinberg 2, D-06120 Halle, Germany

(Received 13 April 1998; accepted for publication 18 November 1998)

It is demonstrated how large-scale arrays of nanomagnets can be efficiently fabricated by shadow deposition onto faceted surfaces of self-organized $Si_{1-x}Ge_x$ films. By pulsed laser deposition of Co in a grazing incidence geometry, we succeeded to cover just one selected type of facets resulting in isolated Co patches with an areal density of about 0.25×10^{12}/in.^{2}. These uniformly oriented nanomagnets have a parallelogram-shaped base with about 25 nm×35 nm edge lengths. Magneto-optic Kerr effect measurements reveal a clear in-plane anisotropy of the nanomagnets. [S0003-6951(99)01004-9]

Within the trend towards ultra-high-density magnetic recording media[1] there are increasing demands for effective and inexpensive ways to fabricate large-area arrays of magnetic nanostructures. The main approach to manufacture arrays of nanomagnets is based on electron-beam lithography that yields structure sizes of less than 50 nm.[2] Besides the low throughput of the method due to the serial processing, it involves a considerable number of technological steps causing high fabrication costs. The second approach—scanning probe microscopy-assisted nanofabrication—uses scanning tunneling microscopy (STM) and atomic-force microscopy (AFM) to create magnetic structures down to the nanoscale.[3] However, these methods are very time consuming and, therefore, hardly suitable for mass production.

An alternative to man-made techniques is to ''let nature do the nanostructuring.'' One way is island formation during growth of magnetic thin films.[4,5] Another way is achieved by utilizing self-assembling or self-organization phenomena to prepare nanostructured substrates, which are then used as templates for subsequent deposition of magnetic material. Size and arrangement of the resulting magnetic particles are determined by the structure of the self-organized substrates. Fe nanostructures have been obtained by electrodeposition into self-organized aluminum oxide pores,[6] thermal growth on a self-assembled $Cu(100)-c(2\times2)N$ surface,[7] or by shadow deposition on self-organized NaCl surfaces.[8] The advantage of this technique is quite obvious: once the self-organized substrate has been prepared only one technological step (i.e., metal deposition) has to be applied. We consider here the strain-induced growth of $Si_{1-x}Ge_x$ films on the technologically relevant Si(001) substrates. For this system a family of self-organized nanostructures has been found,[9] including a surface with just three types of nanofacets.[10] Such a surface is a perfect template to fabricate two-dimensional arrays of nanomagnets because it allows us to cover just one selected facet type under grazing incidence.

In this letter we report on the fabrication of nanomagnets by shadow deposition of Co layers onto the surface of a 2.5 nm $Si_{0.55}Ge_{0.45}$ film grown on a vicinal Si(001) substrate. Figure 1 shows an AFM image of the corresponding $Si_{0.55}Ge_{0.45}$ film surface. The morphology exhibits chains of triangular structures that originate from a step bunch to facet transition occurring at this substrate miscut of 4° towards [110].[10] Analysis of the local surface normals reveals that the surface consists of three types of nanofacets, $(\bar{1}05)$ and $(0\bar{1}5)$ oriented facets and (001) terraces.[10] A model of this surface is presented in Fig. 1(b). The {105} facets are parallelograms with an acute angle of 47° and 25 and 35 nm edge lengths, respectively. The (001) terraces are—for an ideally periodic arrangement of the {105} facets—squares with a size of 35×35 nm^2. With the proper sample orientation one can either deposit on one type of the parallelogram-like {105} facets [see Fig. 1(b)], or on the (100) terraces. In both cases

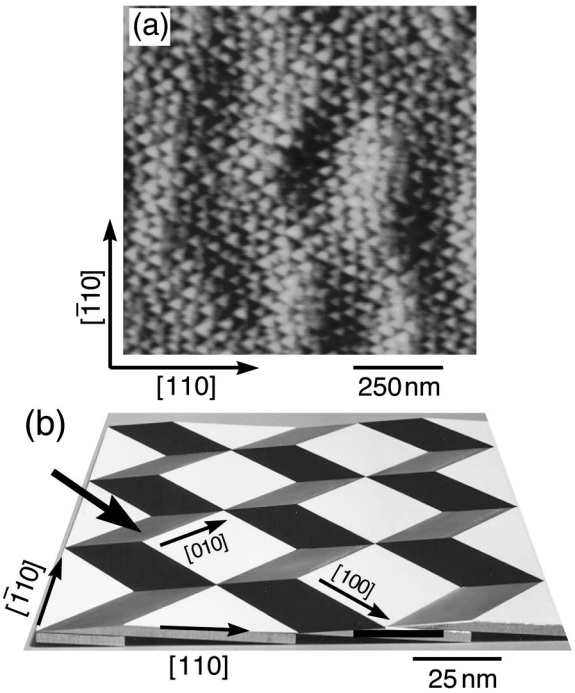

FIG. 1. 2.5 nm $Si_{0.55}Ge_{0.45}$ film grown on a vicinal Si(001) substrate with a 4° miscut towards the [110] direction. (a) Gray-scale AFM image. (b) Three-dimensional model of the surface morphology. The white areas represent (100) terraces, the gray and black areas correspond to $(\bar{1}05)$ and $(0\bar{1}5)$ facets, respectively. The indicated deposition geometry (black arrow) results in an array of parallelogram-like Co patches on the $(\bar{1}05)$ facets.

[a]Present address: Institut für Physik, Montanuniversität Leoben, A-8700 Leoben, Austria. Electronic mail: teichert@unileoben.ac.at

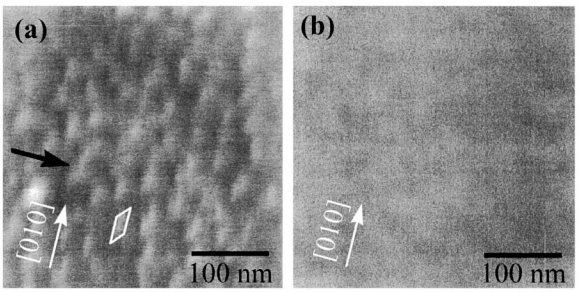

FIG. 2. 360 nm×360 nm SEM images of the template shown in Fig. 1(a) after shadow deposition (a) and normal incidence deposition (b) of a 2 nm Co/2 nm Cu sandwich. The black arrow in (a) denotes the (projected) orientation of the evaporation.

the resulting areal density of the nanomagnets is about 0.25 10^{12}/in.^{2}.

$Si_{1-x}Ge_x$ films were grown under the conditions described in Ref. 9. These films that have a 1 nm native oxide on the surface were covered with Co films of 2 nm thickness (if not otherwise specified) using pulsed laser deposition (PLD) under ultra-high-vacuum conditions. To avoid cobalt silicide formation and oxidation of Co, the film was embedded between two 2 nm Cu films also deposited by PLD. Finally, the samples were capped with a 2 nm Au film. The PLD was performed under conditions that ensure smooth Cu and Co films.[11,12] The angle of deposition was 5° towards the [100] direction of the template, thus exposing only the $(\bar{1}05)$ facets to the Co and Cu sources, respectively.

Figure 2 shows scanning electron microscopy (SEM) micrographs of a sample with a shadow deposited Co film [Fig. 2(a)] and a reference sample that has been prepared under normal incidence resulting in a continuous Co layer [Fig. 2(b)]. While Fig. 2(b) does not show any distinct contrast in SEM, it is the higher secondary electron yield that lets the Co covered $(\bar{1}05)$ nanofacets, i.e., the Co nanomagnets, appear as bright patches in Fig. 2(a). Size, shape, and orientation of the patches correspond to the dimensions of the $(\bar{1}05)$ nanofacets [see the inset in Fig. 2(a)]. The area fraction of the bright patches is 0.25 ± 0.02, which is in excellent agreement with the surface coverage one would expect from the model presented in Fig. 1(b).

Longitudinal magneto-optic Kerr effect (MOKE) measurements were performed to investigate the in-plane magnetization as a function of the azimuthal sample orientation. The accuracy of the azimuthal alignment was ±5° with respect to the [110] cleavage edge. The magnetic field was applied parallel to the macroscopic surface. Hence, a slight tilt up to about 9° may occur between the base planes of the nanomagnets and the field direction. Figure 3 shows magnetization curves for selected sample orientations of both, the shadow deposited samples and a reference sample grown under normal incidence. In order to increase the Kerr signal of the shadow deposited sample, we increased the thickness of the Co film to about 5 nm.[13] In comparison, the shadow deposited films reveal saturation fields in the range of kOe, which is ten times higher than the fields observed for the homogeneous films. Taking into account the 2.5 times larger thickness of the nanomagnets and the 25% surface coverage, we expect for the shadow deposited film a Kerr signal in

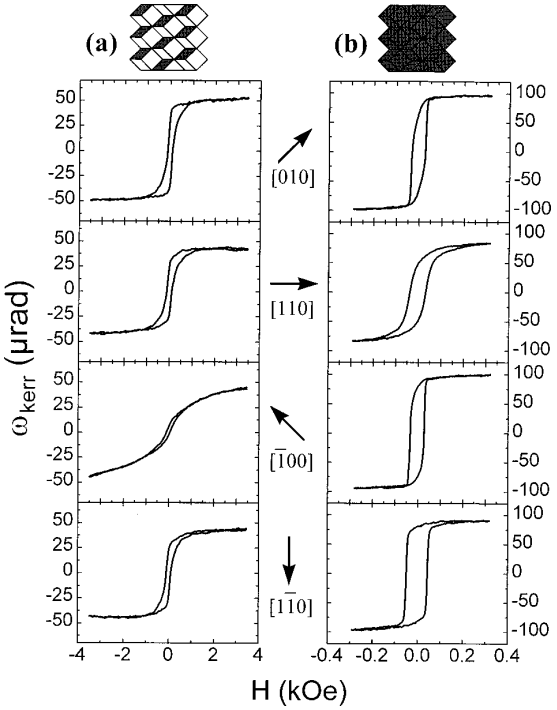

FIG. 3. In-plane hysteresis loops measured by longitudinal MOKE in ⟨100⟩ and ⟨110⟩ orientations. (a) shadow deposition of 5 nm Co onto the Cu covered $(\bar{1}05)$ facets. (b) continuous 2 nm thick Co film prepared by normal incidence deposition. The arrows indicate the orientation of the magnetic field with respect to the nanomagnets or the nanostructured continuous film, respectively. Note the different scales for the magnetic field.

saturation that is roughly 60% of that observed for the continuous film. This value is in rather good agreement with the experimental results along [010].

Besides those deviations a more important finding is manifested in the change of the magnetic anisotropy. While the continuous film has a nearly isotropic magnetic behavior the nanostructured ferromagnets exhibit a strong uniaxial anisotropy. Along the [100] direction an s-shaped hysteresis is found with almost vanishing remanence, whereas the easy axis of magnetization is in [010], i.e., parallel to the long edges of the $(\bar{1}05)$ facets. In Fig. 4 the squareness (ratio of remanence to saturation value) versus the azimuthal orientation of the external field is plotted. In Fig. 4(a), also the theoretical dependence for an ideal uniaxial behavior normalized to the maximum of the experimental results is given. Both the experimental data points and theoretical curve are not corrected for angle deviation of the facet plane to the macroscopic plane of observation, as the correction is small (<2%). Figure 4(a) proves for the nanostructured film the good agreement of the experimental results with the theoretical angle dependence. For the continuous film [Fig. 4(b)], the deviation is so obvious that we omit the theoretical curve. Some uniaxial contribution, however, can be identified in the continuous film as well. The axes of symmetry appear at different directions, with easy and hard axis along [110] and $[\bar{1}10]$, respectively.

In order to find the reason for the uniaxial behavior we have performed worst case estimations for the shape influence on the anisotropy, based on the finite-element method.[14] We obtain for the demagnetizing factor along the facet normal $N_z=0.69$. Within the plane we get values of 0.077 and 0.12 along the [010] and [551] direction, respectively. While

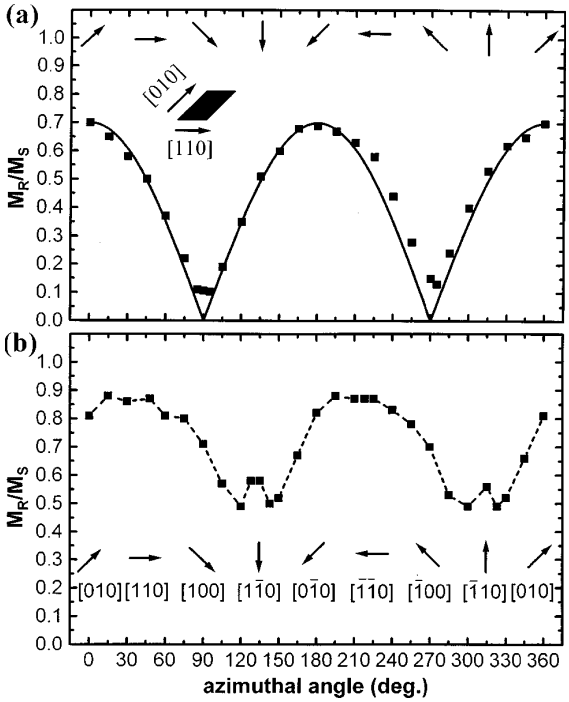

FIG. 4. Squareness (M_R/M_S) of the in-plane hysteresis loops as a function of sample orientation for the shadow deposited sample (a) and the continuous Co film (b). Arrows and the inset are shown to identify the orientation of the magnetic field with respect to the nanostructures for a given azimuthal angle ϕ. The solid line in (a) represents $|\cos(\phi)|$ scaled to the maximum of M_R/M_S.

these numbers support an explanation by shape effects, further investigations of the demagnetization factors in certain in-plane directions rule out that explanation. Due to the asymmetry of the facet with respect to the low index directions of the substrate, the magnetostatic energy for seemingly equivalent directions are unalike. In particular, the shape effects along the [110] and the [$\bar{1}$10] direction of the substrate are different. While the shape anisotropy along [110] is 1.4 times that of the [010] direction, it is 2.8 times larger along [$\bar{1}$10]. The hysteresis loops obtained in these directions, however, are very much the same. From that, we can conclude that the in-plane shape of the nanostructured ferromagnets is not responsible for the anisotropic behavior. The shape effect due to the tilt of the plane of observation to the facet plane can also be neglected. The demagnetization factors are 0.013 and 0.026 for [110] and [100], respectively. Hence, if shape is responsible for magnetic behavior, the anisotropy along [110] should be half that of the hard axis. The hysteresis loop along [110] should exhibit strong deviations from the easy-axis hysteresis, in contradiction to the experimental results.

We do not know the mechanism that makes the (010) direction an easy direction. As the symmetry observed in the experiments [see Fig. 4(a)] does not show a direct correlation to the symmetry of the nanostructure, symmetries on a smaller scale might manifest in the magnetic properties. We might expect that the step structure of the {105} facets[15] is the origin of the uniaxial anisotropy. The ($\bar{1}$05) facets serving as templates for the nanomagnets consist of equally spaced step edges running parallel to the [010] direction producing a uniaxial local symmetry that can cause the uniaxial magnetic property.[16,17] The results obtained with the continuous films also support that hypothesis. The second kind of {105} facets is oriented such that the (100) direction is the easy axis. Hence, for the one {105} facet the easy axis is the direction of hard magnetic behavior of the second one. The system finds the intermediate direction of both facets as the easy axis. This magnetic behavior is not altered by the third kind of facet existing on the self-organized substrate surface, i.e., the fourfold (001) terrace.

The strong increase of the saturation field H_s for the shadow deposited film is striking. This might be due to the effect that the nanomagnets are isolated or only weekly coupled via a narrow stripe along the long diagonals in the shadow deposited films. In any case, the creation of reversed domains, and thus domain walls, is impossible due to the small lateral size of the individual nanomagnet. Thus, one has to assume the magnetization reversal by rotation,[18] which usually happens at higher fields. From our experiments we cannot decide whether the particles switch separately or not.

In summary, we demonstrated that shadow deposition of magnetic material on nanofaceted, self-organized semiconductor substrates is an efficient way to fabricate ultra-high-density arrays of nanomagnets that might be utilized for magnetic storage devices. The self-organized templates used in this study bear the potential of being easily implemented in mainstream semiconductor technology. By varying the deposition angle, there is control of size and separation of the resulting nanomagnets. Moreover, by multistep shadow deposition of material (magnetic and nonmagnetic) onto the different facets, complex magnetic nanostructures as, e.g., giant magnetoresistive devices or sensors can be created.

The authors thank J. C. Bean and L. J. Peticolas for growing the template, M. Füting for recording the SEM micrographs, and W. Lutzke for calculating the demagnetization factors.

[1] See, e.g., Phys. Today **48**, 4 (1995).
[2] S. Y. Chou, P. R. Krauss, and L. Kong, J. Appl. Phys. **79**, 6101 (1996).
[3] A. D. Kent, D. M. Shaw, S. V. Molnar, and D. D. Awschalom, Science **262**, 1249 (1993).
[4] B. Voigtländer, G. Meyer, and N. M. Amer, Phys. Rev. B **44**, 10354 (1991).
[5] T. Jung, R. Schlitter, J. K. Gimzewski, and F. J. Himpsel, Appl. Phys. A: Mater. Sci. Process. **61A**, 467 (1995).
[6] D. AlMawlawi, N. Coombs, and M. Moskovits, J. Appl. Phys. **70**, 4421 (1991).
[7] T. M. Parker, L. K. Wilson, N. G. Gordon, and F. M. Leibsle, Phys. Rev. B **56**, 6458 (1997).
[8] A. Sugawara, G. G. Hembree, and M. R. Scheinfein, J. Appl. Phys. **82**, 5662 (1997).
[9] C. Teichert, M. G. Lagally, L. J. Peticolas, J. C. Bean, and J. Tersoff, Phys. Rev. B **53**, 16334 (1996), and references therein.
[10] C. Teichert, J. C. Bean, and M. G. Lagally, Appl. Phys. A: Mater. Sci. Process. **67A**, 675 (1998).
[11] H. Jenniches, M. Klaua, H. Höche, and J. Kirschner, Appl. Phys. Lett. **69**, 3339 (1996).
[12] Indeed, normal incidence PLD grown Cu/Co/Cu sandwiches coherently cover the self-organized substrate, as was checked by AFM.
[13] Due to the extreme low angle of incidence, the uncertainty of film thickness during shadow deposition was about 20%.
[14] P. Rhodes and G. Rowlands, Proc. Leeds Phil. Liter. Soc. **6**, 191 (1954).
[15] F. Tuinstra, P. M. L. O. Scholte, W. I. Rijnders, and A. J. van den Berg, Surf. Sci. **317**, 58 (1994), and references therein.
[16] A. Berger, U. Linke, and H. P. Oepen, Phys. Rev. Lett. **68**, 839 (1992).
[17] J. Shen and J. Erskine, Phys. Rev. Lett. **68**, 1212 (1992).
[18] A. Aharoni, *Introduction to the Theory of Ferromagnetism* (Clarendon, Oxford, 1996).